The 15th International Symposium on Magnetic Bearings, August 3-6, 2016, Mojiko Hotel, Kitakyushu, Japan

ISMB15

Mechanical design of reconfigurable active magnetic bearing test rig

Eerik SIKANEN*, Rafal P. JASTRZEBSKI**, Pekko JAATINEN**, Teemu SILLANPÄÄ**, Alexander SMIRNOV**, Jussi SOPANEN* and Olli PYRHÖNEN**

* Laboratory of Machine Dynamics, Lappeenranta University of Technology
Skinnarilankatu 34, FI-53851 Lappeenranta, Finland
E-mail: eerik.sikanen@lut.fi

** Laboratory of Control Engineering and Digital Systems, Lappeenranta University of Technology
Skinnarilankatu 34, FI-53851 Lappeenranta, Finland

Abstract

In this study, considerations of a mechanical design of a reconfigurable active magnetic bearing (AMB) test rig and some of its interchangeable modules are reviewed. The manufacturing of modules, assembly, measurements of mechanical accuracies and their influence on electrical and control requirements of the active components are analyzed. Numerical simulations for 10 kW 30000 rpm high-speed rotor of induction motor are performed for studying purposes of rotor dynamics and mechanical stresses of various changeable rotor sleeve parts. Important part of high-speed AMB system are mechanical backup bearings. Additional sub-modules are designed for changeable backup bearings for further rotor dropdown experiments. Also, reference sensors required by the AMB control system are fitted into own sub-module in order to enable testing of various sensor designs. Experimental measurement are performed in order to study rotor dynamics and mechanical accuracies of modular test rig design. Some operational results during commissioning phase are presented and discussed. The benefits and challenges of using a modular design are discussed. The scope of this paper is in mechanical design, therefore no detailed description of designed AMBs and control system is presented.

Key words : Active magnetic bearing, High-speed rotor, Rotor dynamics, Test rig, Reconfigurable, Sub-module design

1. Introduction

High-speed motors equipped with AMBs have a fundamental advantage over conventional motor solutions. AMBs can provide almost frictionless support while allowing the control for the dynamics of the system. Backup bearings are typically used along AMBs in order to avoid damage resulting from a failure. Touchdown can happen because of a failure in any of AMB system hardware components, in the power system, or in the control system. The prototyping of novel solutions as well as modifications or testing of different components and their variants is very challenging in AMB-supported rotor systems.

(Mushi, Lin and Allaire, 2012) made a research focusing on the aerodynamic cross-coupled stiffness forces and uncertain loads of the stability of AMB-supported turbomachinery. In order to excite disturbance in the AMBs, a special exciter is added to the rotor to emulate an impeller and a high pressure oil seal. A belt-drive system was used at maximum operational speed of 15 000 rpm. The Center for Rotating Machinery Dynamics and Control (RoMaDyC) has made multiple publication AMB test rigs and rotor dynamics. In (Kulesza and Sawicki, 2012) transverse shaft crack propagation is studied using rigid finite elements which have been reported to be effective approach in dynamical analysis. (Wroblewski, Sawicki and Pesch, 2012) made interesting research about experimentally driven finite element rotor model optimization based on numerical algorithm of adjusting appropriate finite element model parameters. University of Virginia Rotating Machinery and Controls Laboratory (ROMAC) is known for rotor dynamics and bearing research. (Mushi, Lin and Allaire, 2012) made a research focusing on the aerodynamic cross-coupled stiffness forces and uncertain loads of the stability of AMB-supported turbomachinery. In order to excite disturbance in the AMBs, a special exciter is added to the rotor to emulate an impeller and a high pressure oil seal. A belt-drive system was used at maximum operational speed of 15 000 rpm. (Cloud, 2007) studies rotor stability when supported by tilting pad bearings using test apparatus.

In this study, a mechanical design aspects of a reconfigurable AMB test rig with interchangeable module designs are reviewed. The design and manufacturing verification methods are reviewed. Benefits of interchangeable actuator modules with replaceable reference sensor and backup bearing sub-modules are discussed. Purpose of manufacturing a reconfigurable AMB test rig is to enable component identification, but also design and manufacturing verification. Gathered results during commissioning phase are presented and discussed.

2. Test rig design

The reconfigurable design includes leveled steel base plate and it's fitting to the concrete laboratory machine bed, actuators (motor, AMBs), backup bearing modules, sensor hosting modules and high-speed rotor. The basic configuration of designed and manufactured test rig is presented in Fig. 3. The layout includes radial AMBs with backup bearings on both ends, one axial AMB module and 10 kW 30000 rpm solid rotor induction motor module in the middle (Sikanen, 2014). The main test rig specifications of Configuration I are listed in Tab. 1 and 2. Both finite element method (Borisavljevic, 2013) and analytical approach (Larsonneur, 1990) and (Ranft, 2010) of calculating the mechanics of the high-speed rotor are used. Main benefits of modular design include: possibility to test multiple bearing arrangements, testing different motor or sensor configurations, identification of new components using already identified bearing and sensor modules, mechanical coupling testing and studying multi rotor systems. The bearing modules can easily be repositioned using accurate aligning grooves of the test bench.

Table 1: Rotor and motor specifications

Rotor	
Operational speed	30 000 rpm
Rotor OD	112 mm
Surface velocity	176 m/s
Shaft length	897.5 mm
Mass	17.7 kg
Rotor slits	Curved slits 14 pcs.
Slit width, depth	2.5 mm, 17 mm
Axial AMB disk OD	112 mm
Axial AMB disk	Solid magnetic steel disk
Induction motor	
IM power	10 kW
Stator stack length	80 mm
Stator slots	12 pcs.
IM stator air gap	1.5 mm

Table 2: Bearing and base plate specifications

Bearings	
Radial stator stack length	30 mm
Radial AMB stator	E-core lamination, 12 poles
Radial AMB force	282 N
Radial AMB air gap	1.0 mm
Radial SB air gap	750 µm
Radial SBs	61912 (60-85-13)
Axial AMB stator	Solid magnetic steel stators
Axial AMB force	127 N
Axial AMB air gap	1.0 mm
Axial SB air gap	700 µm
Axial SBs	Brass retainer rings
Base plate and frame structure	
Base plate dimensions	2 500 mm x 300 mm

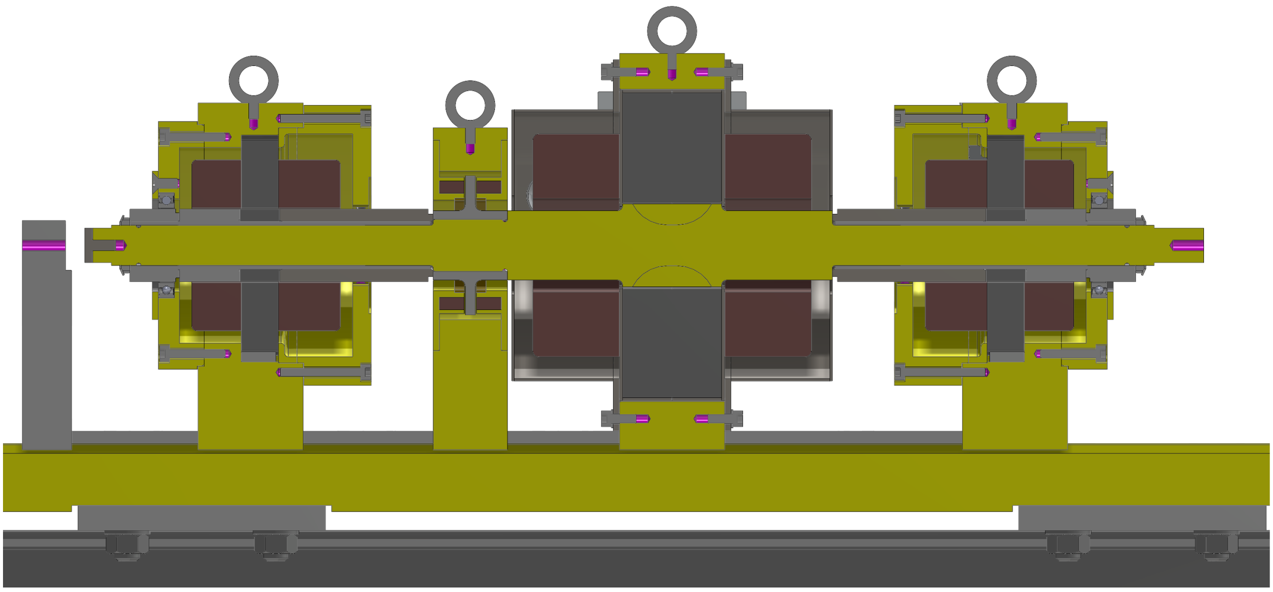

Fig. 1: Cross section of Configuration I test rig

2.1. Reconfigurable design

A multi-sleeve approach was designed to accomplish the reconfigurable rotor design. A secondary requirement for using the sleeve structure is magnetic insulation of rotor active part and AMB laminations. Cross section view of modules and rotor is presented in Fig. 1. The drawback of the multi-sleeve rotor construction has been the increased amount of runout due to tolerance stacking. Rotor dynamic analysis is performed using an in-house developed 3D finite beam element research code in MATLAB. The backup bearing system is designed to be replaceable for rotor dropdown tests; different bearing sizes can be tested by changing the bearing sub-module and the contact sleeve on the rotor, while backup bearing airgap can be varied easily. Due to close proximity between the reference sensors and backup bearings, the sensor data can be easily used to monitor backup bearing performance during rotor dropdown tests.

2.2. Other configurations

Second test rig setup, Configuration II, is similar to first configuration. New design feature is integrated axial and radial AMBs, also called as conical AMBs with permanent magnet biasing in the AMB stators. Third example of designed AMB test rig configuration comprises two PM bearingless motors. In this configuration, one of the main mechanical design aspects discussed is the optimized bridge thickness in the PM rotor active part. Cross sectional view of the rotor stator laminations is presented in Fig. 2. The lamination geometry of 30000 rpm rotating active part is optimized for mechanical durability and electrical performance. In this configuration, the two motor-bearing modules and axial bearing are assembled within a concentric tube providing better accuracy than the separate modules. Detailed description of this design is reviewed in (Jastrzebski et al., 2015) and (Jaatinen et al., 2015). The axial bearing design has been reused from the first configuration.

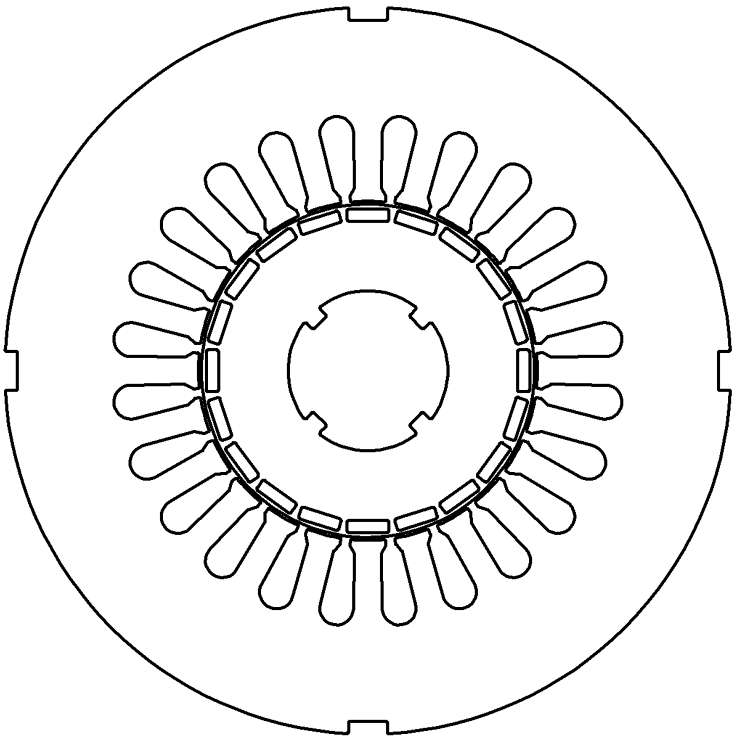

Fig. 2: Cross section of Configuration III bearingless motor

2.3. Backup bearing design

Since backup bearings are considered to be major safety issue in high-speed AMB-supported systems, the backup bearing solution in this reconfigurable test rig is designed to be easily rechangeable for further dropdown and bearing life cycle studying purposes. Special sub-modules for backup bearings are designed and located at the ends of radial AMB modules for easy access. According to (Swanson et al., 2008), main requirements of backup bearing system are: prevent any stator-rotor contacts of active parts, backup bearing must remain operational for adequate life and need to be able to withstand corrosion, vibration and heat. In (Bleuler et al., 2009), many beneficial backup bearing design aspect have been presented. Experimental studies of bearing and contact friction, surface hardness of bearing and rotor sleeve and various damping elements can be studied.

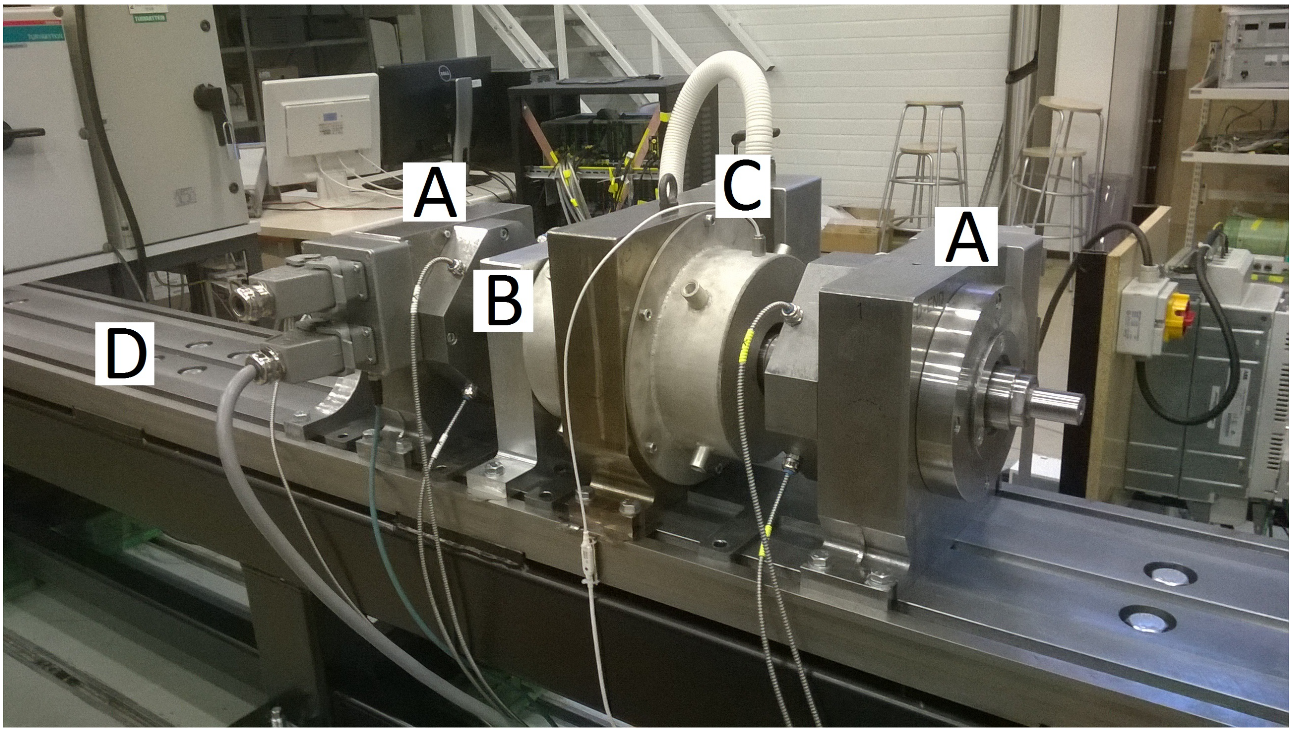

Fig. 3: Exemplary configuration of the assembled AMB test rig during commissioning. Main components of test rig are: A) radial AMB module with detachable sensor and backup bearing sub-modules, B) axial AMB module, C) induction motor stator and D) multipurpose T-slotted test bench.

3. Results

The manufactured AMB test rig is currently under commissioning. So far, the results indicate a reduced positioning accuracy due to the T-rails used as mechanical joints between the modules and test bench. This kind of joint induces always at least minor misalignment. In addition, it was noticed later in commissioning that some of the parts were not manufactured according to the specified tolerances. This was noticed after first tests during commissioning.

3.1. Mechanical accuracies

Test rig module positioning accuracies were identified using a laser position measurement. Accuracies of the module wedge with respect to T-rail in the base plate was measured using Mitutoyo Euro-C 776 Apex coordinate measurement machine. Another device, Leica LTD 500 Laser Tracker, was used to measure the centerline between the modules. Since the base plate is placed on laboratory concrete bench as seen in Fig. 3 minor vertical misalignment in the base plate was notices.

During the laser positioning, the base plate of the test bench was leveled with high accuracy using special regulating legs. Also, the modules were repositioned using thin shim plates to achieve greater lining accuracy. Centerline accuracies before and after repositioning with regulating legs and shim plates are presented in Tab. 3. First and last modules, both radial AMB modules, were used as reference. In order to achieve accurate positioning, the module locations are required to remeasure and reposition if the test rig configuration is changed. After correcting the minor misalignment between the modules and inaccurately manufactured positions wedges in frames, the nominal rotor centerline in respect to the AMB controlling system is in condition.

Table 3: Test rig Configuration I module aligning accuracies before and after realignment

	Drive-end radial AMB	induction motor	axial AMB	non-drive-end radial AMB
	Before realignment			
Y (mm)	0.000	-0.026	0.022	0.000
Z (mm)	0.000	-0.124	0.088	0.000
	After realignment			
Y (mm)	0.000	-0.018	-0.053	0.000
Z (mm)	0.000	-0.022	-0.009	0.000

3.2. Commissioning measurements

The induction motor stator induces minor unbalanced magnetic pull (UMP) which affects to the rotor dynamics. The exact quantity of this force is unknown. Since the test rig configuration is under commissioning it is wise to not induce the system to full speed. Therefore, rotor orbit measurements are performed at relatively low spin speeds. Figure 4 illustrates rotor orbits at radial AMB location at different spin speed from 1000 rpm to 6000 rpm. Most greatest orbital deflections are measured at 2000 rpm. As seen in Fig. 4 orbit size is decreasing while the spin speed is increasing. Depending on the radial AMB stiffness, the noticed great deflection at 2000 rpm speed can be due the rotor rigid body frequency induced with additional magnetic pull of which impact seems to be greatest at low speeds.

Before AMB control system tuning, there were reported problems of failed attempts of trying to initiate rotor levitation while electric motor was powered. The main cause for this problem was large 0.75 mm mechanical backup bearing airgap. Afterwards, backup bearing airgap was reduced to 0.5 mm in order to able radial AMB to generate enough force. Also, the control system loop cycle duration was optimized further. Main cause for UMP may be in stator coils done by manual work.

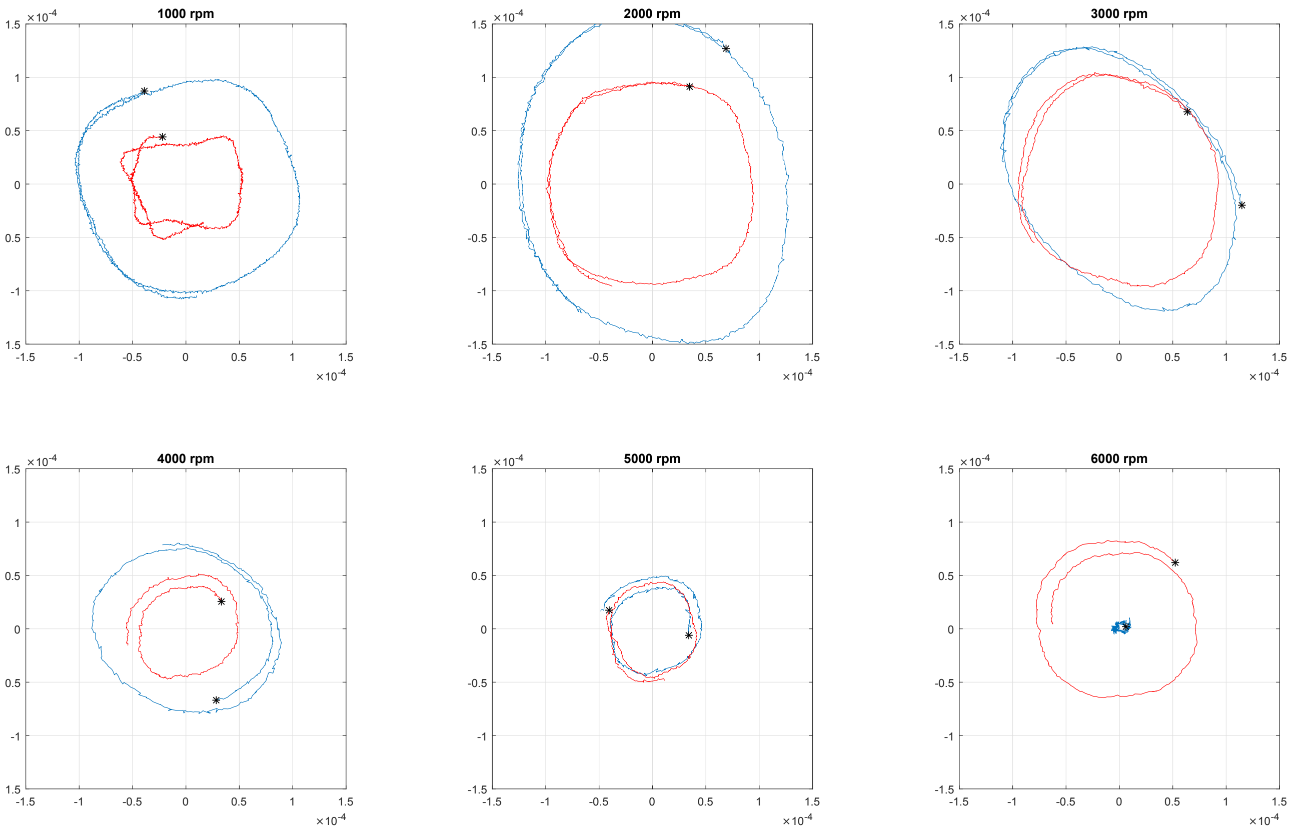

Fig. 4: Measured rotor orbits (in m) at radial AMB locations at different spin speeds, blue curve represents drive-end and red curve non-drive-end, black dot represents starting points

Due to modular design, a relatively high radial air gap of 0.75 mm of the AMBs is applied. The manufacturing tolerances of the sensor sleeve surfaces and the tolerances used for the active bearing surfaces cause respective runouts, which have been measured for non-polished rotor. The problems in the multi-sleeve structure have since been revised for new rotors to be manufactured for Configuration II and Configuration III.

Real measured clearance center points of radial AMB modules are presented in Fig. 5 as green dots. The Ctr values in Fig. 5 indicate the real combined affect of electrical and mechanical accuracies measured. During initial levitation a contact to reference sensor was accidentally occurred. In Fig. 5 this contact is clearly visible as a segment of backup bearing clearance is unreachable. Also, effect of gravity with additional UMP may cause reduction of AMB force in this particular direction. Since this, the sensor clearances have been recalibrated and backup bearing airgaps have been reduced by replacing the backup bearing sleeves in the rotor construction.

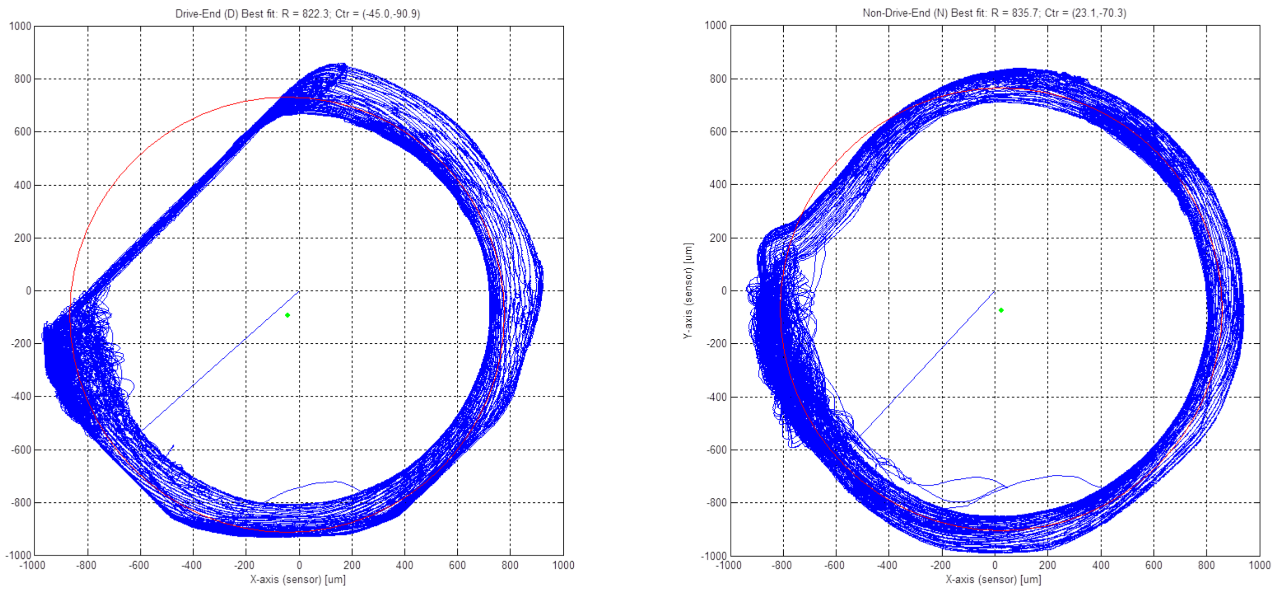

Fig. 5: Measured backup bearing orbit at early stage of commissioning

3.3. High-speed induction machine rotor design

The eigenfrequencies of the designed high-speed rotor of induction motor are simulated using in-house made MATLAB based rotor dynamics simulation tool using finite 3D Timoshenko beam element. For comparison purposes the same rotor is modeled in ANSYS using finite solid elements.

Based on Experimental Modal Analysis (EMA), the free body eigenfrequencies of real rotor were measured using Scanning Laser Doppler Vibrometer (SLDV). When using experimentally measured eigenfrequencies as reference, the finite element models were tuned to match these frequencies as closest as possible. In literature, it is suggested (Lantto, 1997) to use reduced, even zero elastic modulus to shrink fitted sleeve parts. Therefore, the model tuning was performed by varying the elastic modulus of shrink fitted rotor sleeve parts and axial AMB disk. Table 4 presents the results of tuned rotor models. EMA is performed to non-rotating rotor, then the impact of gyroscopic effect can be neglected. Additional shrink fitted sleeve stress studies (Ranft, 2010) were performed in order to achieve proper tolerances.

Table 4: Results of rotor eigenfrequency studies

	1. mode		**2. mode**	
Measured	259.4 Hz		550.0 Hz	
Beam 1 % *E*	195.4 Hz	-24.7 %	382.9 Hz	-30.4 %
Beam 20 % *E*	259.0 Hz	-0.2 %	579.8 Hz	5.4 %
Beam 50 % *E*	303.1 Hz	16.8 %	749.2 Hz	36.2 %
Solid 1 % *E*	201.9 Hz	-22.2 %	380.5 Hz	-30.8 %
Solid 20 % *E*	268.4 Hz	3.5 %	576.3 Hz	4.8 %
Solid 50 % *E*	307.9 Hz	18.7 %	743.9 Hz	35.3 %

Differences between modeling method appears. First of all, the model constructed using beam elements does not take into account the axial forces caused by the tightening torque of the spinner nuts or the radial forces caused by the shrink fits. In the solid element model, frictional contacts with a friction coefficient of 0.2 was used. In the beam element model, the shrink fitted parts are defined as additional hollow elements over the main shaft elements with reduced material properties. Therefore, the contacts with friction between parts are not accounted for when using beam element approach.

4. Conclusions

In this study, the mechanical design considerations and results of designing and commissioning of a reconfigurable AMB test rig are presented. Capabilities of modular structure are revealed. Selected results during the commissioning are presented and discussed. Imperfections of mechanical tolerances and further required modification during system assembly are discussed. Noticeable runout during initial levitation of Configuration I is reported and since has been fixed. Further research topics related to this test rig design were discussed.

References

Bleuler, H., Schweitzer, G. and Maslen, E. H., Magnetic Bearings: Theory, Design, and Application to Rotating Machinery, Springer, (2009).

Cloud, C. H., Stability of Rotors Supported by Tilting Pad Journal Bearings, Dissertation, University of Virginia, (2007).

Borisavljevic, A., Limits, Modeling and Design of High-Speed Permanent Magnet Machines, Dissertation, Delft University of Technology, (2013).

Jaatinen, P., Jastrzebski, R. P., Sugimoto, H., Pyrhönen, O. and Chiba, A., Optimization of the rotor geometry of a high-speed interior permanent magnet bearingless motor with segmented magnets, 18th International Conference on Electrical Machines and Systems (ICEMS) (2015), pp.962–967.

Jastrzebski, R. P., Jaatinen, P., Sugimoto, H., Pyrhönen, O. and Chiba, A., Design of a bearingless 100 kW electric motor for high-speed applications, 18th International Conference on Electrical Machines and Systems (ICEMS) (2015), pp.2008–2014.

Kulesza, Z. and Sawicki J. T., New Finite Element Modeling Approach of a Propagating Shaft Crack, Journal of Applied Mechanics, (2012).

Lantto, E., Finite Element Model for Elastic Rotating Shaft, Licentiate thesis, Acta Polytechnica Scandinavica, Electrical Engineering Series, (1997).

Larsonneur, R., Limits, Design and Control of Active Magnetic Bearing Systems for High Speed Rotation, Dissertation, Swiss Federal Institute of Technology Zürich, (1990).

Mushi, S. E., Lin, Z. and Allaire, P. E., Design, Construction, and Modeling of a Flexible Rotor Active Magnetic Bearing Test Rig, IEEE/ASME Transactions on Mechatronics, Vol.17, No.6 (2012), pp.1170-1182.

Ranft, C. J. G., Mechanical Design and Manufacturing of a High Speed Induction Machine Rotor, Dissertation, North-West University, Potchefstroom Campus, (2010).

Sikanen, E., Mechanical Design and Analysis of Modular Active Magnetic Bearing Test Rig, Master's thesis, Lappeenranta University of Technology, (2014).

Swanson, E. E., Maslen, E. H., Li, G. and Cloud, C. H., Rotordynamic Design Audits of AMB Supported Machinery, Proceedings of the Thirty-Seventh Turbomachinery Symposium, (2008).

Wroblewski, A. C., Sawicki, J. T., and Pesch, A. H., Rotor Model Updating and Validation for an Active Magnetic Bearing Based High-Speed Machining Spindle, Journal of Engineering for Gas Turbines and Power, Vol. 134, No.12, (2012), pp.122509.